Order, disorder and dynamics in brownmillerite $Sr_2Fe_2O_5$

Josie E. Auckett[†#*], Wai Tung Lee[‡], Kirrily C. Rule[‡], Alexey Bosak[§] and Chris D. Ling[†]

[†]School of Chemistry, The University of Sydney, Sydney 2006, Australia

[#]Department of Chemistry, Durham University, Durham DH1 3LE, United Kingdom

[‡]Australian Centre for Neutron Scattering, Australian Nuclear Science and Technology Organisation, Lucas Heights 2234, Australia

[§]European Synchrotron Radiation Facility, BP 220, 38043 Grenoble Cedex, France

Supporting Information Placeholder

ABSTRACT: The room-temperature structure of brownmillerite-type $Sr_2Fe_2O_5$ remains controversial, despite numerous published crystallographic studies utilising x-ray, neutron and electron diffraction data collected on single-crystalline and powder samples. The main disagreements concern the ordering of twisted FeO_4 tetrahedral chains within and between the layers stacked along the *b* axis, and the impact of this ordering on oxide-ionic conductivity. Here, we present new data along with a reinterpretation of previously published diffraction images, including the re-assignment of satellite reflections, which harmonise the results of past studies in a unified description of tetrahedral chain ordering in $Sr_2Fe_2O_5$ at length scales relevant to x-ray and neutron diffraction. Implications for the prevailing model of oxide ion transport in this material are also discussed.

INTRODUCTION

The brownmillerite oxides ($A_2B_2O_5$, *A* = alkali earth, *B* = transition or Group 3 metal) have been widely studied over many decades for their diverse properties, which include fast ionic conductivity[1-4], thermoelectricity[5], catalytic activity[6-7] and complex magnetic ordering[8-9]. The structure is derived from the archetypical cubic perovskite by removal of parallel ⟨110⟩ rows of oxygen atoms to yield alternating layers of BO_6 and BO_4 units arranged in corner-linked sheets and chains, respectively (Figure 1(a)). Oxide-ionic conductivity has been observed and characterised in several brownmillerite phases, though many of these exhibit a sharp increase in conductivity upon conversion to a cubic perovskite phase with disordered oxygen vacancies at high temperatures,[1, 4, 10] suggesting that the best performance may be achieved by suppressing the low-temperature brownmillerite phase. Nevertheless, the mechanism of oxide-ionic transport in the brownmillerite structure continues to attract significant interest.[3, 11-12]

The majority of detailed structural and dynamic studies of brownmillerites have focused on the relative inter- and intralayer arrangements of oppositely twisted "L"- and "R"-type BO_4 chains, which determine the unit cell symmetry. The most commonly reported ordering schemes involve no intralayer variation, with neighbouring layers either like-oriented (*Ibm*2) or oppositely-oriented (*Pcmn*; Figure 1). These "simple" brownmillerite structures, along with the fully chain-disordered *Icmm* model, define an orthorhombic unit cell that is related to the perovskite lattice parameter a_P ≈ 3.9 Å by $a \approx c \approx \sqrt{2}\cdot a_P$, $b \approx 4\cdot a_P$. Numerous crystallographic studies conducted since 2001 have established the existence of more complicated ordering schemes that can be described generally using the superspace group $I2/m(\alpha\beta0)0s$ with a modulation vector, $\mathbf{q} = \alpha\mathbf{a}^* + \beta\mathbf{b}^*$,[13] in which the α and β parameters reflect intra- and interlayer chain ordering sequences, respectively. Commensurate versions of this modulation are often represented as three-dimensional supercells.[13] Attempts to rationalise the adoption of different chain-ordering schemes in brownmillerites were first made by Abakumov *et al*.[14-15] and later expanded upon by Parsons *et al*.[16], who noted that inter- and intralayer chain type alternation may be energetically favourable due to compensation of the opposite dipole moments of the L and R chains. However, the proximity of oppositely twisted chains correlates with an increase in unfavourable structural "disruption" (distortion and tilting) within the octahedral layers, resulting in an energetic competition whose outcome is influenced by geometric parameters such as the interlayer spacing and degree of chain twisting.[16]

The various brownmillerite chain-arrangement models are generally difficult to distinguish by x-ray diffraction (XRD), because their differences chiefly concern the positions of light oxygen atoms, which make a weak relative contribution to the scattered x-ray signal in the presence of heavier metallic elements. Studies utilising neutron powder diffraction (NPD) data, which tends to suffer inherently from lower signal-to-noise ratios and poorer angular resolution, have yielded similarly inconclusive results.[17-18] Although the *Pcmn* structure can be positively identified in many cases due to its lack of *I*-centring extinction conditions, the distinction between the *Icmm* and *Ibm*2 models is often marginal, and the satellite reflections arising from modulated oxygen ordering schemes are virtually impossible to identify without access to single-crystal samples.

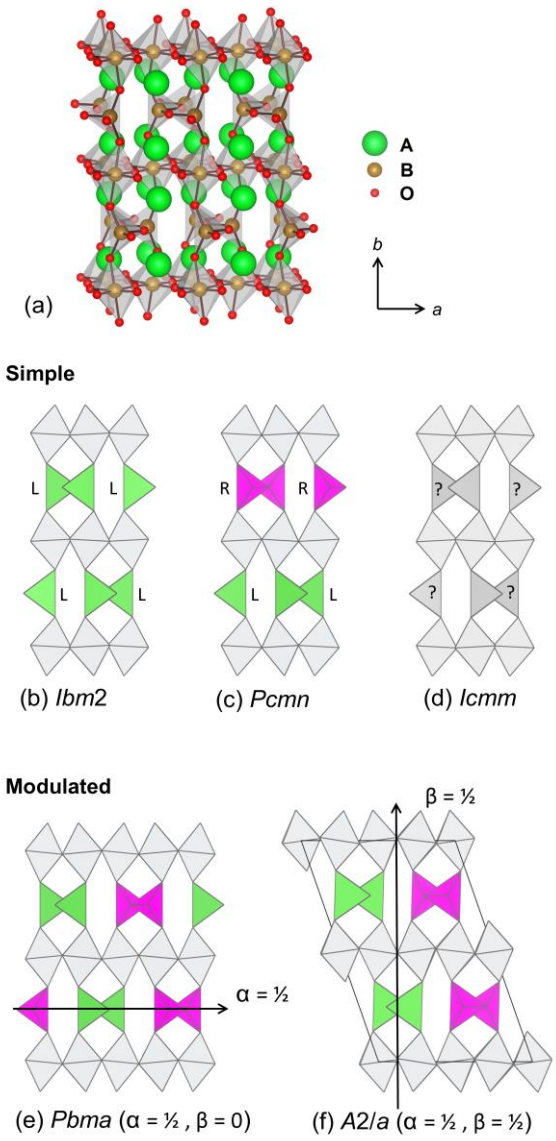

Figure 1. (a) The general brownmillerite structure consisting of BO_6 octahedra and BO_4 tetrahedra in alternating layers. (b-f) Polyhedral representations of tetrahedral chain-ordering schemes in brownmillerite. Images b-d depict the three simplest brownmillerite structure types, in which the tetrahedral chains adopt simple order (*Ibm*2 or *Pcmn* symmetry) or statistical disorder (*Icmm* symmetry). Images e and f show examples of supercells generated by commensurate chain-ordering modulations. The effects of the α and β parameters are illustrated.

One of the most persistently controversial brownmillerite structures is that of $Sr_2Fe_2O_5$, for which moderate ionic conductivity has been reported.[1] The phase was first identified as a brownmillerite in 1964 by Gallagher *et al*., who assigned the space group *Pcmn* by analogy to $Ca_2Fe_2O_5$.[19] Subsequent diffraction studies re-assigned the space group of $Sr_2Fe_2O_5$ to either *Icmm*[17, 20] or *Ibm*2[18, 21], although most authors noted that the assignment of their chosen model was uncertain. In 2008, an electron diffraction study revealed several different types of modulated order in microscopic $Sr_2Fe_2O_5$ crystallites (including regions of *Pbma*- and *A*2/*a*-type commensurate order),[13] and concluded that the disordered *Icmm* model provided a reasonable approximation to the long-range average structure while the ordered *Ibm*2 model was unequivocally wrong. The presence of modulated order in $Sr_2Fe_2O_5$ was further supported by subsequent neutron diffraction studies on single-crystals grown by the floating-zone method, which were reportedly dominated by the commensurate (α = ½, β = 0) *Pbma* superstructure on the length scale of neutron diffraction.[11, 22] The *Pbma* structure was also found to be the thermodynamic ground state of $Sr_2Fe_2O_5$ by density functional theory (DFT) calculations.[23] However, the *Icmm* long-range approximation was claimed to be more consistent with the results of a synchrotron x-ray diffraction experiment on small (~70 μm) fragments of similarly grown crystals.[12]

In the present work, we attempt to harmonise the results of all recent studies of single-crystal samples using neutron[11, 22], x-ray[12] and electron[13] diffraction data. Re-examining these results in light of new data presented in the following sections, we show that the best average description of tetrahedral chain ordering in $Sr_2Fe_2O_5$ is achieved by the *Pbma* model with disordered stacking faults, which captures the most important features of all published data and also agrees with theoretical calculations.[23] Importantly, while this entails re-assigning some reflections in references 22 and 11, it does not alter the consistency of those data with our model.

EXPERIMENTAL SECTION

The growth of $Sr_2Fe_2O_5$ crystals by the optical floating-zone (FZ) method and subsequent single-crystal monochromatic neutron diffraction experiments are described elsewhere.[22]

In order to distinguish clearly between reflections arising from nuclear and magnetic scattering, additional polarised neutron diffraction data were collected on the same FZ-grown crystal rod using the thermal triple-axis neutron spectrometer TAIPAN[24] at the OPAL research reactor, ANSTO, Australia. Two polarised ^{3}He spin-filter cells were used, one acting on the incident beam as a polariser and the other on the diffracted beam as an analyser. Data were collected near several Bragg reflections in the twinned (010)/(102) plane of the FZ-grown $Sr_2Fe_2O_5$ crystal rod at room temperature. Initial test data were collected with a magnetic guide field applied perpendicular to the diffraction plane. Additional data were collected using a Pastis coil to rotate the guide field with respect to the sample. Measured intensities were corrected for time-dependent polarisation decay using the procedures described by Wildes.[25] Exploratory data collected in both spin-flip modes, (+−) and (−+), yielded no evidence for magnetic chirality in $Sr_2Fe_2O_5$, therefore the (−+) data were omitted from all subsequent data collection runs.

Single-crystal synchrotron diffraction data were collected at the MX1 beamline of the Australian Synchrotron using the ADSC Quantum 210r area detector. The sample was a fragment ~10 μm on edge that was chipped from the FZ-grown crystal. An incident energy of 17.500 keV (λ = 0.71070 Å) was used. Samples were attached to a pin mount using Paratone oil and maintained at a temperature of 100 K in a nitrogen cryostream throughout the experiment. Diffraction image frames were collected for 1 s at 1° intervals for a full 360° rotation about the horizontal mounting axis. In order to investigate the presence of weak features, particularly diffuse scattering, an additional data set with deliberately over-saturated reflection intensities was collected at room temperature on a ~50 μm crystal fragment at the ID23 beamline of the European Synchrotron Radiation Facility (ESRF) in Grenoble,

France, using an incident x-ray wavelength of λ = 0.77490 Å. These diffraction images were collected for 0.1 s at 0.1° sample rotation intervals, with the data binned into 0.2° rotation intervals for visualisation and data reduction. Three-dimensional visualisation, indexing and reduction of all synchrotron diffraction data was performed using CrysAlis^{PRO}.

Simulated neutron and x-ray diffraction patterns were generated for various $Sr_2Fe_2O_5$ structure models using the Jana2006 software.[26]

RESULTS AND DISCUSSION

All unit cell indexing hereafter refers to the *Pbma* brownmillerite supercell depicted in Figure 1(d) with dimensions $a \approx 2\sqrt{2}\cdot a_P$, $b \approx 4\cdot a_P$, $\approx c \approx \sqrt{2}\cdot a_P$, except where the *B* subscript is used to denote the simple brownmillerite unit cell with undoubled *a* axis.

Twinning in $Sr_2Fe_2O_5$ crystals

The growth of single-crystal $Sr_2Fe_2O_5$ from the molten phase during the floating-zone (FZ) growth process is hindered by the phase transition from orthorhombic brownmillerite to cubic perovskite between 700–875 °C.[18, 27-28] The stoichiometric high-temperature phase contains 1/6 oxygen vacancies distributed randomly over the perovskite lattice, and is believed to persist up to the melting point of $Sr_2Fe_2O_5$. As the FZ-grown cubic perovskite crystal cools through this phase transition, the considerable strain imposed across its very large (mm²) cross-section is relieved by the adoption of a micro-twinned arrangement of orthogonal brownmillerite domains.[22] Given the structural relationship between the cubic perovskite ($a_P \approx 3.9$ Å) and unmodulated orthorhombic brownmillerite ($a \approx c \approx \sqrt{2}a_P$, $b \approx 4a_P$) unit cells, the crystallographic directions in brownmillerite (B) which correspond to ⟨100⟩-type directions in perovskite are $\langle 010\rangle_B$ and $\langle 101\rangle_B$, yielding a total of twelve possible unique orientations of the orthorhombic cell in relation to any fixed $[100]_P$-based twin axis.[12] However, in space groups having rotational symmetry elements about the *b* axis, pairs of twins separated by 180° rotations about *b* are equivalent and only six twin types need to be considered (Figure 2). The only commonly-encountered brownmillerite variant for which all twelve twins are unique is the *Ibm*2 model containing all like-oriented chains. However, as electron diffraction has already established that $Sr_2Fe_2O_5$ does not adopt this symmetry,[13] the twelve-twin scheme will not be discussed further here.

Magnetic reflections in neutron diffraction data

The first studies of a FZ-grown crystal of $Sr_2Fe_2O_5$ used monochromatic neutron diffraction images obtained for a large (cm-scale) portion of the crystal boule. These data were indexed using only four of the six possible twin orientations.[11] The four twins comprised two orientation pairs related by rotations around $[010]_B$, such as A and D, B and E in Figure 2. It was therefore possible to identify one of the three orthogonal $\langle 100\rangle_P$-type directions in the crystal boule which contained no $[010]_B$ component of any twin.

"Satellite" reflections identified at the $(h, 2k+1, h)_B$ positions in neutron precession images were previously used to justify the *a*-doubled *Pbma* chain-ordering model for $Sr_2Fe_2O_5$.[22] These reflections were not considered to be magnetic in origin by the authors[11] because they persisted to high *Q* values and temperatures >100 °C above the well-established Néel temperature of $Sr_2Fe_2O_5$ (~400 °C)[18, 29]. However, the same reflections were not observed in x-ray precession images obtained from a different crystal specimen by Maity *et al.*[12] Recalculated neutron diffraction maps presented in Figure 3 confirm that the *k*-odd reflections of all twin components in this plane are in fact reproduced in both the *Icmm* subcell and *Pbma* supercell models when magnetic scattering from the G-type antiferromagnetic (AFM) structure of $Sr_2Fe_2O_5$[18, 29] is included. Neither model accounts for the reflections when magnetic scattering is not included.

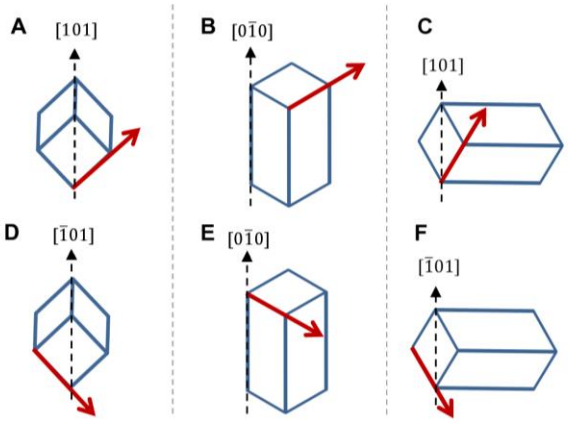

Figure 2. Six possible orientations of a simple brownmillerite unit cell with rotational symmetry about *b* when twinned along its perovskite $\langle 100\rangle_P$-type directions, which correspond to $\langle 010\rangle_B$ and $\langle 101\rangle_B$ in the brownmillerite cell. Solid red arrows indicate the positive [100] direction and dashed black arrows identify the vertical direction in each cell.

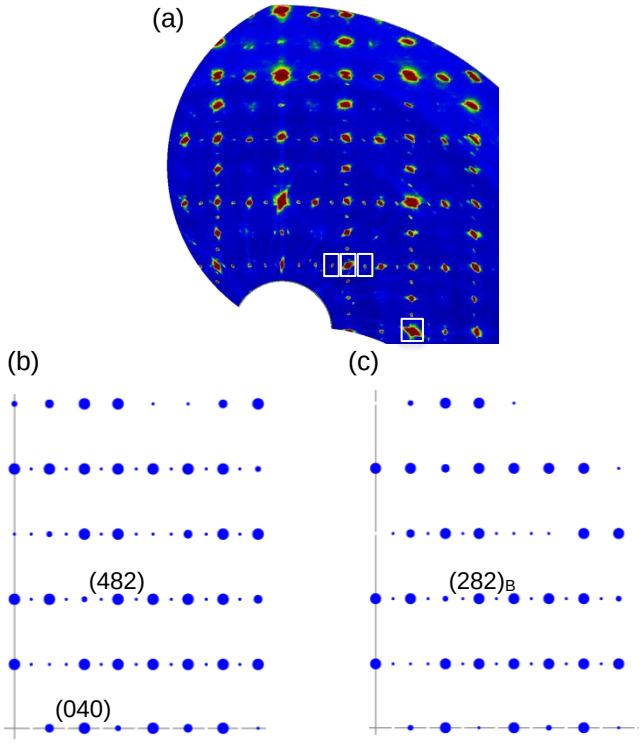

Figure 3. (a) Monochromatic neutron diffraction data collected for $Sr_2Fe_2O_5$ at room temperature (reproduced from Ref. 22, Figure 3). White boxes indicate reflections selected for polarised neutron diffraction measurements in this work. (b) Simulated diffraction pattern for one twin component with G-type antiferromagnetic spin ordering (μB = 4.5 per

Fe^{3+} ion[29]) parallel to *c* in the *Pbma* supercell. (c) The same simulation using the *Icmm* subcell.

We have now confirmed the magnetic origin of the $(h, 2k+1, h)_B$ reflections in the measured twin plane experimentally by polarised neutron diffraction data collected on the same FZ-grown crystal used in Ref. 11. Spin-flip (SF) and non-spin-flip (NSF) measurements of the (231) and (251) reflections in one twin component of the crystal plane are presented in Figure 4, along with the non-magnetic (080) and (241) reflections for comparison. The (++) and (– –) peak intensities obtained in a perpendicular guide field (H ⊥ *q*) were approximately equal to each other for all four reflections, indicating either purely nuclear or purely magnetic scattering, but the significant SF intensity observed for (231) and (251) unambiguously confirms their magnetic nature. The ratios of (++) to (+–) intensities recorded in the perpendicular guide field indicate that the *B* site magnetic moments are inclined out of the scattering plane at an angle of ~45° to [201], consistent with the known AFM ordering model for $Sr_2Fe_2O_5$ with spins aligned in the *c* direction. Further details of the magnetic scattering analysis can be found in the Supporting Information.

Confirmation of the observed $(h, 2k+1, h)_B$ or $(2h, 2k+1, h)$ reflections as purely magnetic contradicts the earlier claim[22] that the appearance of these reflections in Figure 3(a) supported the existence of the *Pbma* supercell in $Sr_2Fe_2O_5$. However, the diffraction image in the perpendicular plane (presented in the same article, Figure 4 and in Ref. 11, Figure 2) contains many well-resolved superstructure reflections that cannot be indexed using a brownmillerite subcell, as they would correspond to non-integer $(h_B+½)$ indices. This is discussed further in the following section.

Single crystal synchrotron x-ray diffraction studies

Single-crystal diffraction data collected from ~10^{-5} m diameter crystal fragments at the ID23 (room temperature) and MX1 (100 K) beamlines were indexed independently using the automated peak searching and cell indexing functions available in CrysAlis^{PRO}. In both cases, the indexing routine identified two primitive orthorhombic lattices whose dimensions agreed well with the lattice parameters of the *Pbma* brownmillerite supercell identified in Ref. 22. The reciprocal lattices of the two cells were related by an 88.5° rotation around *b** and can thus be assigned to Twins A and D as defined in Figure 2.

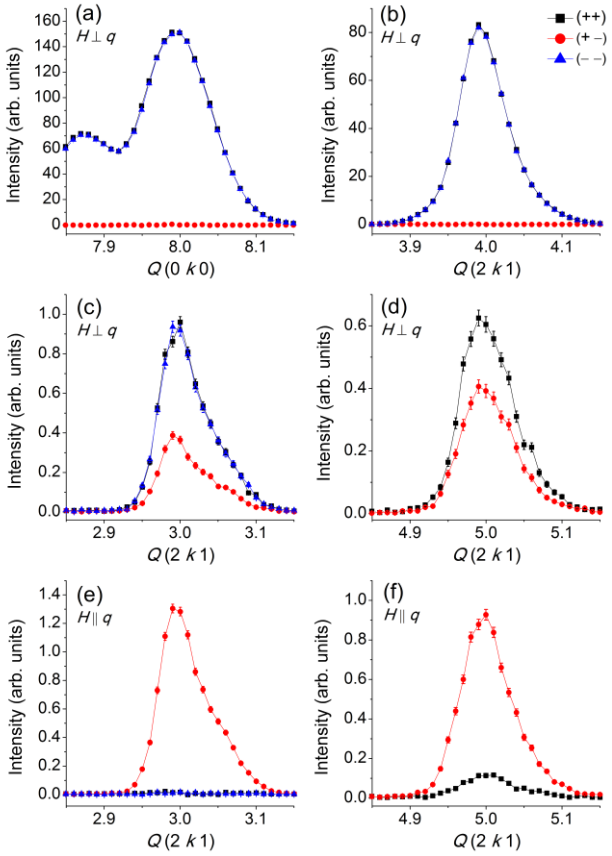

Figure 4. Polarised neutron diffraction data collected in SF (+–) and NSF (++), (– –) modes near various reflections in the FZ-grown single crystal of $Sr_2Fe_2O_5$. Scans were made near the (a) (080), (b) (241), (c) (231) and (d) (251) reflections in a perpendicular guide field, and repeated near (e) (231) and (f) (251) in a parallel guide field. Error bars are drawn on all plots and are smaller than symbols in (a) and (b). Lines are a guide to the eye.

Table 1. Unit cell details for three twin components indexed to single-crystal synchrotron x-ray diffraction data collected for $Sr_2Fe_2O_5$.

	Lattice type	*a* (Å)[a]	*b* (Å)[a]	*c* (Å)[a]	% refl. matched[b]	unique % matched[c]
ID23						
1	orthorhombic *P*	11.3273	15.5784	5.5509	67.6	31.4
2	orthorhombic *P*	11.3283	15.5821	5.5552	56.6	20.6
3	orthorhombic *I*	5.5823	15.8005	5.5437	42.3	6.1
MX1						
1	orthorhombic *P*	11.3459	15.4955	5.52303	40.0	30.7
2	orthorhombic *P*	11.3409	15.4977	5.5216	43.9	34.6

[a]Standard deviations are not reported by CrysAlis^{PRO} for the lattice parameters of multiple twins indexed simultaneously, but single-cell searches typically yielded uncertainties in the order of 10^{-4}–10^{-3} Å. [b]Percentage of the whole data set indexed by the cell, including overlaps. [c]Percentage of reflections matched exclusively by that cell.

A third cell, comprising an *I*-centred orthorhombic lattice with approximate dimensions of a simple brownmillerite and oriented like an orthogonal twin component in Figure 2 (e.g. Twin B), was identified among the remaining unmatched reflections in the ID23 data set. The lattice parameters of this twin were somewhat different to the corresponding dimensions of Twins A and D, but this is probably due to the fact that only a small percentage of the peaks matched by the third domain were unique to it, and the majority of reflections used for its determination overlapped with the other twin component lattices with which it was imperfectly aligned. The existence of *a*-doubling satellite reflections in the lattice of Twin B, analogous to Twins A and D, could not be ruled out due to the weak diffraction signal from this twin. No additional unit cells were identified in the MX1 data set, which utilised a smaller crystal fragment (~10 μm on edge). From these observations we conclude that the length scale of [010]-related microtwinning in FZ-grown $Sr_2Fe_2O_5$ is smaller than that of the twinning on $[101]_B$, as the 10–50 μm specimens appear to contain roughly equal volumes of two [010]-paired twins but achieve partial or full elimination of the other, orthogonal [010]-pair that was present in neutron diffraction images of the FZ-grown crystal rod.[22] Notably, the slightly larger (~70 μm) crystal used by Maity *et al.*[12] also contained the four twins observed in the bulk rod, suggesting that this scale represents an approximate lower bound for the interleaving of orthogonal [010] twin pairs in FZ-grown crystals of $Sr_2Fe_2O_5$.

Structure refinements were not performed against either synchrotron diffraction data set due to the difficulty of obtaining satisfactory corrected intensities for large numbers of overlapping reflections. Precession images reconstructed from the MX1 data were compared visually with diffraction maps calculated for the *Pbma* and *Icmm* structure models. The "(*hk*o)" plane (defined with respect to Twin A, and also containing (o*kl*) of twin D) and the "(o*kl*)" plane (containing (*hk*o) of twin D) images were both described adequately using the simple *Icmm* model (Supplementary Figure S3), but several other planes showed unambiguous *h*-odd reflections arising from *Pbma*-type cell doubling (Figure 5).

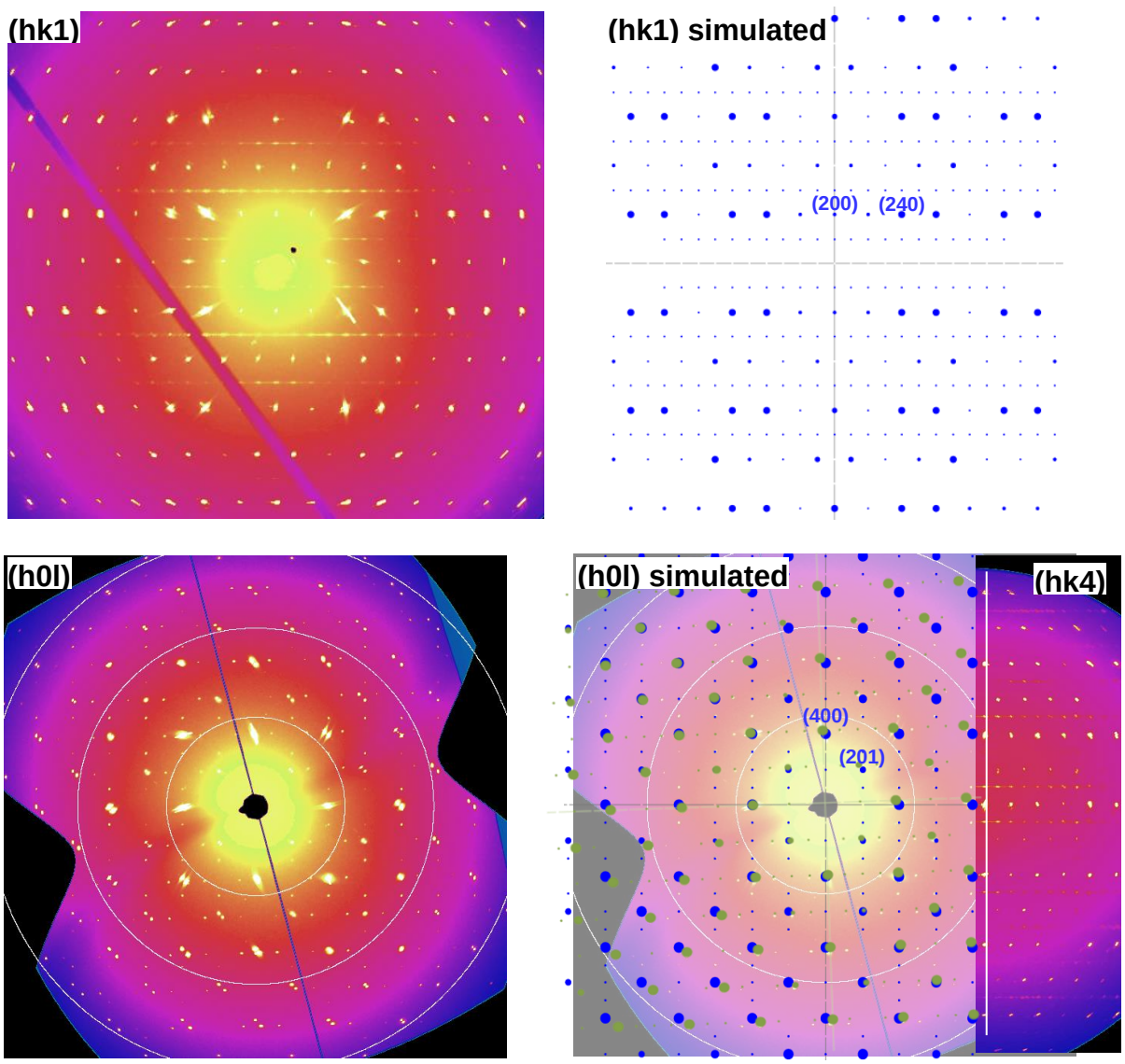

Figure 5. Synchrotron x-ray precession images shown with patterns simulated for the *Pbma* model of $Sr_2Fe_2O_5$. Plane labels refer to the blue twin component. In (b), the white line indicates the perpendicular intersection of the (*hk*4) inset plane with (*h*o*l*).

The "(*hol*)" image (Figure 5(b)) corresponds to the diffraction plane depicted in Figure 5 of Maity *et al.*,[12] in which a virtually identical twinned pattern of reflections is observed, including the weak *h*-odd reflections attributed to the doubled cell of the *Pbma* model. The authors contended that these features do not constitute evidence for a doubling of the *a* lattice parameter, because they arise from the intersection of perpendicular rods of diffuse scattering intensity with the diffraction plane. Such rods are frequently observed in single-crystal studies of brownmillerites, including in the present work (Figure 5), and are attributed to disordered stacking faults along the *b* axis.[13, 30-31] However, it should be noted that the presence of a one-dimensional diffuse feature in reciprocal space corresponds to two-dimensional order in an intersecting perpendicular plane. Therefore, these well-defined, one-dimensional diffuse rods intersecting the $(hol)_B$ brownmillerite plane at $h = n + ½$ indices are an indication of well-defined order along *a*, which does effectively double that lattice parameter. The physical interpretation in $Sr_2Fe_2O_5$ is that the tetrahedral chains exhibit strict intralayer L-R-L-R order along *a*, but disorder along *b* due to imperfect stacking of these ordered layers.[13, 31] In the context of competition between dipole moment compensation and structural distortion described by several authors,[14-16] we take this to mean that the chain-dipole magnitude in $Sr_2Fe_2O_5$ is large enough to induce intralayer anti-correlations between neighbouring dipoles (chains), but not large enough to overcome the interlayer spacing and enforce strict alignment between successive layers. The local stacking of layers is therefore susceptible to disruption by even minor fluctuations in the thermal conditions during sample preparation, and is expected to vary within and between samples. This scenario is mentioned explicitly by Parsons *et al.* as one possible form of disorder manifested by the brownmillerite phases in the "*Imma*" region of their structural variant map (Figure 12 of their paper), this being the region into which $Sr_2Fe_2O_5$ was classified.[16]

The energetic preference for dipole-cancelling L-R-L-R intralayer sequencing in $Sr_2Fe_2O_5$ is also supported by the DFT calculations of Young and Rondinelli, which found the *Pbma* structure to be lower in energy than either of the homogeneous-intralayer *Ibm*2 and *Pcmn* structures with which it was compared.[23]

Because no conventional three-dimensional unit cell can be constructed to properly represent the one-dimensional disorder outlined above, we believe that the best description of the structure at macroscopic length scales is achieved using the ordered *Pbma* (or *C*2/*c*) model while acknowledging the presence of disordered stacking faults. This description is consistent with all modern single-crystal x-ray and neutron diffraction studies[11-12, 22] and represents an average of the local ordering schemes observed by D'Hondt *et al.* in different microscopic regions of their sample (*i.e.*, variable β but consistent $\alpha \approx 1/2$).[13]

The completely chain-disordered *Icmm* model provides a less appropriate description of the average structure of $Sr_2Fe_2O_5$ for two reasons. Firstly, this model implies completely free tetrahedral chain disorder in two dimensions, and fails to capture the strict L-R-L-R correlations that are maintained within each layer. For similar reasons, some authors of prior studies have proposed modifications of ordered models to capture partial or imperfect ordering in brownmillerite phases, such as the *Ibm*2 model with large anisotropic displacement parameters used to describe "a small amount of disorder" in $(La_{1-x}Ba_x)_2Mn_2O_5$,[16] or the two-component mixture of *Ibm*2 and *Pcmn* phases refined against powder XRD data in order to model microdomains and stacking faults in $Ca_2MnGaO_{5+\delta}$.[32] Secondly, the *Icmm* model allows the possibility of both static and dynamic chain disorder, whereas strict intralayer order implies that any interlayer disorder (arising from stacking faults) is primarily static in nature (unless entire layers of alternating chains were capable of switching their orientations concertedly and rapidly, which is highly unlikely). The implications of this conclusion for ionic conductivity in $Sr_2Fe_2O_5$ are discussed in the next section.

Implications for the dynamic behaviour of $Sr_2Fe_2O_5$

Although the *Pbma* structure assigned on the basis of neutron diffraction data in Refs. 22 and 11 was justifiable, some magnetic *k*-odd reflections were incorrectly identified in both papers as nuclear reflections arising from the *a*-doubling of the brownmillerite unit cell. The most significant consequence of this misidentification was the incorrect analysis of the temperature dependence of superstructural ordering, as depicted in Figure 3 of Ref. 11. Revisiting the same variable-temperature neutron diffraction data set reveals that a row of true *h*-odd superstructure reflections, present in an adjacent diffraction layer, persist virtually unchanged up to the highest recorded temperature (725 °C) (Figure 6). Any significant disordering of the brownmillerite tetrahedral chains sufficient to destroy the dominant long-range intralayer order must therefore occur above this temperature, *i.e.*, almost 200 °C higher than previously reported.

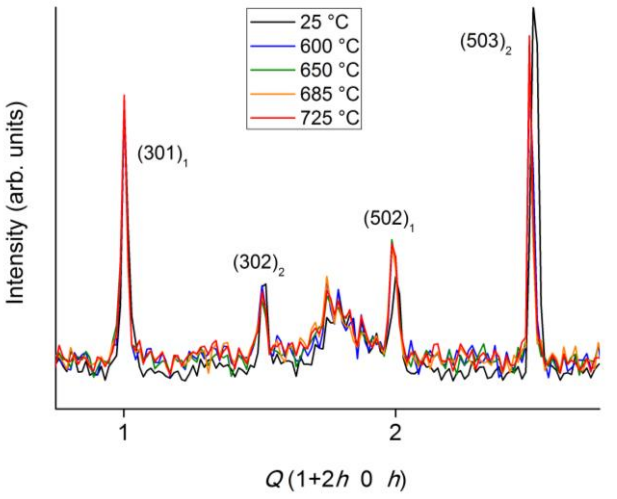

Figure 6. Integrated satellite reflections in layer 1 of the monochromatic neutron diffraction data for $Sr_2Fe_2O_5$. Subscripts (1 or 2) indicate reflections arising from different twin components. The *x* axis scale refers to twin component 1. The broad feature arises from the tail of the very intense (402)/(080) reflection in an adjacent layer bleeding into the integration strip.

The presence and persistence of strict tetrahedral chain order up to the temperature range where ionic conductivity is observed is critical to the interpretation of experimental data and any discussion of ion-diffusion mechanisms in $Sr_2Fe_2O_5$. Paulus *et al.*[3] proposed a mechanism in which the

"apical" oxide ions (*i.e.* those at the shared corners of octahedra and tetrahedra) migrate into the vacancy rows between the tetrahedral chains and diffuse along the *c* axis (designated *a* in that work), facilitated by dynamic switching of the orientations of adjacent tetrahedral chains whose gate-like motions shuttle the ions along the row. This dynamic reorientation of chains – even at room temperature – was supported by density functional theory-based molecular dynamics (DFT-MD) at a simulation temperature of 350 K, which also reproduced the hopping of apical oxide ions into the vacancy channels. The authors further asserted that the long-range structure of $Sr_2Fe_2O_5$ is best described as chain-disordered (*Icmm* symmetry), and that any additional disorder is dynamic.[3, 12] However, we have shown above that disruption of long-range intralayer chain order does not occur to any significant degree at room temperature. Indeed, the electron diffraction work of D'Hondt *et al*.[13] alone is sufficient to demonstrate this, as even the relatively short-range structure modulations reported in that study would not be observable in the event of wholesale dynamic switching of the tetrahedral chains. The DFT-MD results presented in Ref. 3 are therefore seen to contradict the crystallographic evidence. The most likely source of the discrepancy is the nominal temperature of the simulations. We note that comparable DFT-MD simulations reported in Ref. 11 identified very similar dynamic behaviour, but at very different temperatures, with apical oxide-ion displacements and tetrahedral chain disordering absent at 300 °C but clearly observed at 600 °C – *i.e.* hundreds of degrees higher than previously reported simulations, yet still beneath the lower limit for significant chain disordering as evidenced by Figure 6. Nominal temperatures in DFT-MD simulations are known to be qualitatively unreliable, and the effective temperatures at which phenomena occur in DFT-MD simulations often deviate significantly from experimental observations. In the case of $Sr_2Fe_2O_5$, the simulations should be especially sensitive to the *b* parameter, which determines the apical Fe–O bond lengths and hence the strength of binding interactions between the apical oxide ions and the octahedral Fe.

Despite showing that dynamic chain-switching is implausible at moderate temperatures, we do not discount other published evidence that suggests the apical oxide ions participate in oxide ion conductivity. Experimental and calculated inelastic neutron scattering (INS) spectra identified a phonon mode at 7 meV associated with apical Fe–O vibrations which merged with low-energy acoustic branches at 800 °C; the same mode in the non-conductive brownmillerite $Ca_2Fe_2O_5$ was observed at considerably higher energies.[3] Furthermore, broadening of quasielastic neutron scattering (QENS) signals (indicative of fast ion diffusion) have been observed experimentally at 750 °C[11] and 800 °C[3] but not at 600 °C; therefore, we cannot rule out dynamic chain disordering commencing between 725 and 750 °C. Finally, we note that oxide ion conduction in $Sr_2Fe_2O_5$ is not necessarily incompatible with the retention of intralayer chain order; the apical oxide ions could perhaps diffuse along the vacancy channels facilitated by reorientation of only a few local tetrahedra without disrupting the overall chain orientation, or without assistance from the chains at all. Mean-square displacement maps calculated from DFT-MD simulations in Ref. 11 indicate dominant two-dimensional oxygen motion within the tetrahedral layers of the *a*-*c* plane rather than one-dimensional motion along *c* only, suggesting that strictly directional diffusion of the mobile ions along well-defined channels between tetrahedral chains is not the primary mechanism of transport in the brownmillerite structure.

CONCLUSIONS

Apparent conflicts between published diffraction data and their structural interpretations can be resolved by considering $Sr_2Fe_2O_5$ as a partially chain-ordered brownmillerite which exhibits strict L-R-L-R intralayer order combined with interlayer disorder along the *b* axis. The most appropriate model for $Sr_2Fe_2O_5$ on macroscopic length scales is therefore a commensurate brownmillerite supercell in *Pbma* with disordered stacking faults. The *Icmm* model incorporating full chain disorder provides a less-apt description of $Sr_2Fe_2O_5$, and should only be applied as a simple structural approximation in cases where local structural detail is not essential to the matters under discussion.

Pbma-type intralayer chain ordering in $Sr_2Fe_2O_5$ persists to at least 725 °C, *i.e.*, almost 200 °C higher than previously reported. Nevertheless, the mechanism of oxide ion mobility proposed for $Sr_2Fe_2O_5$ remains largely compatible with the revised structure model. Evidence in the literature for apical oxide ions diffusing along the corner-connected tetrahedral rows or more freely in the tetrahedral plane remains valid, with the axial octahedral Fe–O bond length and strength appearing to influence the activation energy. However, the degree of chain reorientation facilitating this diffusion must be considered in light of strict intralayer order being maintained even above the onset temperature of appreciable ionic conductivity. We hope that the clarification of the optimal local and long-range descriptions of tetrahedral chain order in $Sr_2Fe_2O_5$ will inform further investigations into its structural and dynamic behaviour in the context of understanding ionic conductivity mechanisms in brownmillerites.

ASSOCIATED CONTENT

Supporting Information

Theory and further discussion of polarised neutron diffraction analysis; additional synchrotron x-ray single-crystal diffraction images from MX1 and ID23 experiments.

AUTHOR INFORMATION

Corresponding Author

*josie.auckett@durham.ac.uk

Author Contributions

All authors have given approval to the final version of the manuscript.

Funding Sources

J.E.A. acknowledges funding and support from an Australian Institute of Nuclear Science and Engineering (AINSE) Postgraduate Research Award and a Royal Society Newton International Fellowship. C.D.L. acknowledges funding from the Australian Research Council (DP110102662).

ACKNOWLEDGMENT

The authors wish to thank Assoc. Prof. Michael Gardiner (University of Tasmania) for facilitating the MX1 experiment, and Dr Jason Price (Australian Synchrotron) for invaluable

assistance with the conversion and visualisation of the MX1 data sets.

REFERENCES

(1) Leonidov, I. A.; Patrakeev, M. V.; Bahteeva, J. A.; Poholok, K. V.; Filimonov, D. S.; Poeppelmeier, K. R.; Kozhevnikov, V. L. Oxygen-ion and electron conductivity in $Sr_2(Fe_{1-x}Ga_x)_2O_5$. *J. Solid State Chem.* **2006,** *179* (10), 3045-3051.

(2) Boivin, J. C.; Mairesse, G. Recent material developments in fast oxide ion conductors. *Chem. Mater.* **1998,** *10* (10), 2870-2888.

(3) Paulus, W.; Schober, H.; Eibl, S.; Johnson, M.; Berthier, T.; Hernandez, O.; Ceretti, M.; Plazanet, M.; Conder, K.; Lamberti, C. Lattice Dynamics To Trigger Low Temperature Oxygen Mobility in Solid Oxide Ion Conductors. *J. Am. Chem. Soc.* **2008,** *130* (47), 16080-16085.

(4) Berastegui, P.; Hull, S.; García-García, F. J.; Eriksson, S. G. The crystal structures, microstructure and ionic conductivity of $Ba_2In_2O_5$ and $Ba(In_xZr_{1-x})O_{3-x/2}$. *J. Solid State Chem.* **2002,** *164* (1), 119-130.

(5) Asenath-Smith, E.; Lokuhewa, I. N.; Misture, S. T.; Edwards, D. D. p-Type thermoelectric properties of the oxygen-deficient perovskite $Ca_2Fe_2O_5$ in the brownmillerite structure. *J. Solid State Chem.* **2010,** *183* (7), 1670-1677.

(6) Hirabayashi, D.; Yoshikawa, T.; Mochizuki, K.; Suzuki, K.; Sakai, Y. Formation of brownmillerite type calcium ferrite ($Ca_2Fe_2O_5$) and catalytic properties in propylene combustion. *Catal. Lett.* **2006,** *110* (3-4), 269-274.

(7) Yang, Y.; Cao, Z. Q.; Jiang, Y. S.; Liu, L. H.; Sun, Y. B. Photoinduced structural transformation of $SrFeO_3$ and $Ca_2Fe_2O_5$ during photodegradation of methyl orange. *Mater. Sci. Eng., B* **2006,** *132* (3), 311-314.

(8) Brotzeller, C.; Geick, R.; Marchukov, P.; Rudashevsky, E. G.; Balbashov, A. M. Magnetic Excitations in Dicalcium Ferrite. *Solid State Commun.* **1992,** *82* (11), 923-925.

(9) Maljuk, A.; Strempfer, J.; Lin, C. T. Floating zone growth and characterization of $Ca_2Fe_2O_5$ single crystals. *J. Cryst. Growth* **2003,** *258* (3-4), 435-440.

(10) Shin, J. F.; Orera, A.; Apperley, D. C.; Slater, P. R. Oxyanion doping strategies to enhance the ionic conductivity in $Ba_2In_2O_5$. *J. Mater. Chem.* **2011,** *21* (3), 874-879.

(11) Auckett, J. E.; Studer, A. J.; Pellegrini, E.; Ollivier, J.; Johnson, M. R.; Schober, H.; Miiller, W.; Ling, C. D. Combined Experimental and Computational Study of Oxide Ion Conduction Dynamics in $Sr_2Fe_2O_5$ Brownmillerite. *Chem. Mater.* **2013,** *25* (15), 3080-3087.

(12) Maity, A.; Dutta, R.; Penkala, B.; Ceretti, M.; Letrouit-Lebranchu, A.; Chernyshov, D.; Perichon, A.; Piovano, A.; Bossak, A.; Meven, M.; Paulus, W. Solid-state reactivity explored *in situ* by synchrotron radiation on single crystals: from $SrFeO_{2.5}$ to $SrFeO_3$ via electrochemical oxygen intercalation. *J. Phys. D: Appl. Phys.* **2015,** *48* (50), 504004.

(13) D'Hondt, H.; Abakumov, A. M.; Hadermann, J.; Kalyuzhnaya, A. S.; Rozova, M. G.; Antipov, E. V.; Van Tendeloo, G. Tetrahedral Chain Order in the $Sr_2Fe_2O_5$ Brownmillerite. *Chem. Mater.* **2008,** *20* (22), 7188-7194.

(14) Abakumov, A. M.; Kalyuzhnaya, A. S.; Rozova, M. G.; Antipov, E. V.; Hadermann, J.; Van Tendeloo, G. Compositionally induced phase transition in the $Ca_2MnGa_{1-x}Al_xO_5$ solid solutions: Ordering of tetrahedral chains in brownmillerite structure. *Solid State Sci.* **2005,** *7* (7), 801-811.

(15) Hadermann, J.; Abakumov, A. M.; D'Hondt, H.; Kalyuzhnaya, A. S.; Rozova, M. G.; Markina, M. M.; Mikheev, M. G.; Tristan, N.; Klingeler, R.; Büchner, B.; Antipov, E. V. Synthesis and crystal structure of the $Sr_2Al_{1.07}Mn_{0.93}O_5$ brownmillerite. *J. Mater. Chem.* **2007,** *17* (7), 692-698.

(16) Parsons, T. G.; D'Hondt, H.; Hadermann, J.; Hayward, M. A. Synthesis and Structural Characterization of $La_{1-x}A_xMnO_{2.5}$ (A = Ba, Sr, Ca) Phases: Mapping the Variants of the Brownmillerite Structure. *Chem. Mater.* **2009,** *21* (22), 5527-5538.

(17) Hodges, J. P.; Short, S.; Jorgensen, J. D.; Xiong, X.; Dabrowski, B.; Mini, S. M.; Kimball, C. W. Evolution of oxygen-vacancy ordered crystal structures in the perovskite series $Sr_nFe_nO_{3n-1}$ (n=2, 4, 8, and ∞), and the relationship to electronic and magnetic properties. *J. Solid State Chem.* **2000,** *151* (2), 190-209.

(18) Schmidt, M.; Campbell, S. J. Crystal and magnetic structures of $Sr_2Fe_2O_5$ at elevated temperature. *J. Solid State Chem.* **2001,** *156* (2), 292-304.

(19) Gallagher, P. K.; Buchanan, D. N.; MacChesney, J. B. Mössbauer Effect in the System $SrFeO_{2.5-3.0}$. *J. Chem. Phys.* **1964,** *41* (8), 2429-2434.

(20) Greaves, C.; Jacobson, A. J.; Tofield, B. C.; Fender, B. E. F. A Powder Neutron Diffraction Investigation of the Nuclear and Magnetic Structure of $Sr_2Fe_2O_5$. *Acta Crystallogr., Sect. B: Struct. Sci.* **1975,** *31* (MAR15), 641-646.

(21) Harder, M.; Müller-Buschbaum, H. Preparation and Investigation of $Sr_2Fe_2O_5$ Single Crystals - A Contribution to Solid State Chemistry of $M_2Fe_2O_5$ Compounds. *Z. Anorg. Allg. Chem.* **1980,** *464* (5), 169-175.

(22) Auckett, J. E.; Studer, A. J.; Sharma, N.; Ling, C. D. Floating-zone growth of brownmillerite $Sr_2Fe_2O_5$ and the observation of a chain-ordered superstructure by single-crystal neutron diffraction. *Solid State Ionics* **2012,** *225*, 432-436.

(23) Young, J.; Rondinelli, J. M. Crystal structure and electronic properties of bulk and thin film brownmillerite oxides. *Phys. Rev. B* **2015,** *92* (17), 174111.

(24) Danilkin, S. A.; Horton, G.; Moore, R.; Braoudakis, G.; Hagen, M. The TAIPAN thermal triple-axis spectrometer at the OPAL reactor. *J. Neutron Res.* **2007,** *15* (1), 55-60.

(25) Wildes, A. R. The polarizer-analyzer correction problem in neutron polarization analysis experiments. *Rev. Sci. Instrum.* **1999,** *70* (11), 4241-4245.

(26) Petříček, V.; Dušek, M.; Palatinus, L. Crystallographic Computing System JANA2006: General features. *Z. Kristallogr.* **2014,** *229* (5), 345-352.

(27) Grenier, J. C.; Ea, N.; Pouchard, M.; Hagenmuller, P. Structural Transitions at High Temperature in $Sr_2Fe_2O_5$. *J. Solid State Chem.* **1985,** *58* (2), 243-252.

(28) Shin, S.; Yonemura, M.; Ikawa, H. Order-Disorder Transition of $Sr_2Fe_2O_5$ from Brownmillerite to Perovskite Structure at an Elevated Temperature. *Mater. Res. Bull.* **1978,** *13* (10), 1017-1021.

(29) Takeda, T.; Yamaguchi, Y.; Watanabe, H.; Tomiyoshi, S.; Yamamoto, H. Crystal and Magnetic Structures of $Sr_2Fe_2O_5$. *J. Phys. Soc. Jpn.* **1969,** *26* (5), 1320.

(30) Istomin, S. Y.; Abdyusheva, S. V.; Svensson, G.; Antipov, E. V. Synthesis, crystal and magnetic structure of a novel brownmillerite-type compound Ca2Co1.6Ga0.4O5. *J. Solid State Chem.* **2004,** *177* (11), 4251-4257.

(31) Krüger, H.; Stöber, S.; Welberry, T. R.; Withers, R. L.; Gerald, J. D. F. Stacking faults and superstructures in a layered brownmillerite. *Acta Crystallogr., Sect. B: Struct. Sci.* **2011,** *67*, 476-485.

(32) Abakumov, A. M.; Rozova, M. G.; Pavlyuk, B. P.; Lobanov, M. V.; Antipov, E. V.; Lebedev, O. I.; Van Tendeloo, G.; Sheptyakov, D. V.; Balagurov, A. M.; Bouree, F. Synthesis and crystal structure of novel layered manganese oxide Ca_2MnGaO_{5+d}. *J. Solid State Chem.* **2001,** *158* (1), 100-111.

For Table of Contents only

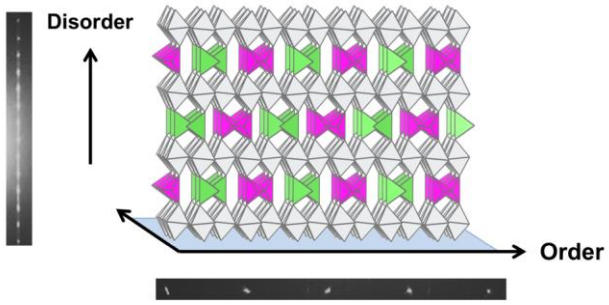

Tetrahedral chains in layered brownmillerite-type $Sr_2Fe_2O_5$ adopt locally ordered arrangements within each layer up to temperatures near the onset of oxide-ionic conductivity (>600 °C). Imperfect layer stacking results in a two-dimensionally ordered, one-dimensionally disordered model which provides the most appropriate structural description of $Sr_2Fe_2O_5$.